JOURNAL OF GEOPHYSICAL RESEARCH, VOL. 106, NO. C9, PAGES 19,797–19,807, SEPTEMBER 15, 2001

On the decay of a baroclinic jet flowing along a continental slope

Robert Hetland[1]
Woods Hole Oceanographic Institution, Woods Hole, Massachusetts

Ya Hsueh
Department of Oceanography, Florida State University, Tallahassee, Florida

Dongliang Yuan
Science Systems and Applications, Inc., Lanham, Maryland

Abstract. A jet flowing in the Kelvin wave propagation direction along the seaward side of a continental slope is found to decrease in strength as it leaks mass onto the continental shelf. As a result, a shelf break jet flowing in the opposite direction is induced on the shelf. The combination of these two flows creates a decaying, high-pressure tongue centered about the shelf break. An idealized, reduced gravity model is developed to examine the two-flow combination. In the model a baroclinic open ocean jet flows next to a continental shelf over which the flow is barotropic and dominated by a linear bottom friction proportional to along-shelf velocity. The far-field depth of the thermocline is assumed to be much greater than the depth of the shelf break. A solution is found in the limit of small cross-slope flow. The mathematical problem of finding the flow on the shelf is equivalent to that of heat conduction on a semi-infinite rod with a finite heat source placed at the end of the rod. A numerical shelf/slope junction model is devised to allow the requirement of small cross-slope flow to be relaxed. The numerical model, which incorporates higher-order dynamics, confirms the qualitative results obtained from the analytic model. The motivation for the development of the theory lies in observational evidence of a northward flowing jet along the continental slope off the West Florida Shelf, apparently stemming from the Loop Current. The structure of the flow combination over the shelf break is confirmed with historical hydrographic data and advanced very high resolution radiometer imagery.

1. Introduction

Circulation on the outer continental shelf is driven mainly by forcing from the deep ocean. Many shelf circulation models that examine offshore influence have used periodic forcing at some point seaward of the shelf break [*Welsh*, 1986]. In fact, numerical solutions of free shelf waves often exploit the fact that periodic forcing offshore excites resonance in pressure over the shelf at the various shelf wave modal frequencies [*Chapman and Brink*, 1987]. Others have used specified sea level gradients at the shelf break in simple geometries to get analytical solutions of the shelf flow [*Csanady*, 1978; *Middleton*, 1987]. However, in all of these models the offshore pressure is prescribed and the pressure distribution on the shelf is solved with respect to the predetermined pressure forcing.

A notable exception is the work by *Chapman* [1986], where a steady state, frictional, barotropic flow model over a continental shelf and slope is constructed with a shelf flow specified at some "initial" point along the shelf while keeping the deep ocean at rest. The structure of this steady state flow is examined as it evolves in the Kelvin wave propagation direction, the "downstream" direction of influence spreading. The continental shelf is found to act as an insulator for the spreading of the pressure field [*Csanady and Shaw*, 1983; *Chapman and Brink*, 1987; *Shaw and Peng*, 1987]. A pressure front is found to develop at the shelf break, creating a jet. A like approach is taken here in examining a similar flow structure over the West Florida Shelf (WFS). The difference in the present case is that the specified jet is set just seaward of the continental slope and that the shelf is considered at rest at the initial upstream point. As the pressure field develops downstream, the pressure in the deep ocean can modify, and be modified by, the evolving pressure field over the shelf.

1.1. Motivation

The WFS is a wide shelf in the northeastern Gulf of Mexico, in which the open ocean circulation is dominated by the Loop Current with quasiperiodical ring separation [*Sturges*, 1992, 1994]. While the nearshore (shoreward of the ~50-m isobath) portion of the WFS exhibits flows that are primarily wind driven, the considerably broad outer shelf region admits influence from the Loop Current [*Li and Weisberg*, 1999].

Recent studies [*Hetland*, 1999; *Hetland et al.*, 1999] have uncovered a strong southward jet just shoreward of the shelf break. The southward flowing jet appears to be driven by an offshore pressure distribution generated as the Loop Current

[1]Now at Department of Oceanography, Texas A&M University, College Station, Texas.

Paper number 2000JC000254.
0148-0227/01/2000JC000254$09.00

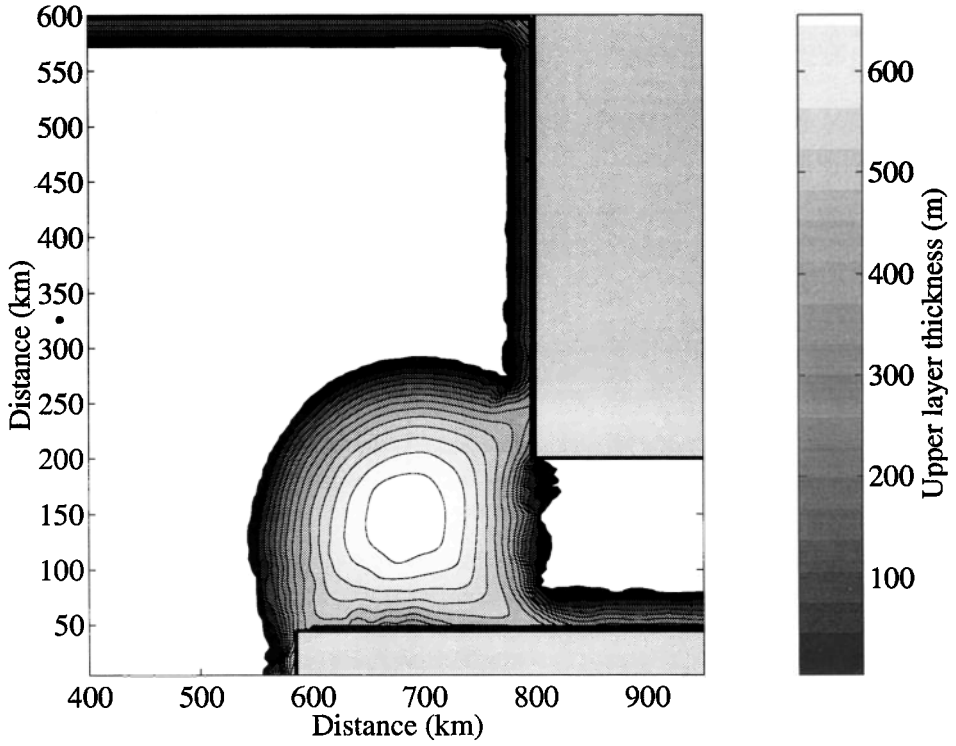

Figure 1. Output from the reduced gravity numerical model, 80 days into the simulation. Parameters used are $\Delta\rho/\rho_0 = 0.01$, $f = 6.16 \times 10^{-5}$ s^{-1}, and $\beta = 2.07 \times 10^{-11}$ m s^{-1}, which are representative of the Gulf of Mexico.

makes contact with the shelf. The pressure is high at the point of contact because it is a stagnation point and is low to the south because the Loop Current is constricted and Flow speed increases. The high extends to the north with diminishing strength, following a small northward flowing branch created by the contact. The high-pressure tongue has also been found in the output of a numerical model designed to study the circulation in the northeastern Gulf of Mexico (Y. Hsueh and Y. Golubev, A note on the Flow in DeSoto Canyon in response to northerly wind bursts in winter, submitted to *Gulf of Mexico Science*, 2001, hereinafter referred to as Hsueh and Golubov, submitted manuscript, 2001). The northward decrease in pressure suggests a broad, onshore flow over the length of the shelf at the shelf break that feeds the southward flowing jet inshore of the shelf break.

A primary goal of the present study is to understand the dynamics of this onshore flow or, in other words, to understand the dynamics of the decaying high-pressure tongue along the shelf break. This endeavor involves examining the evolving interrelationship between the shelf and oceanic pressure fields along the shelf break. To the lowest order, the West Florida Slope acts as an insulator to the oceanic pressure influence and may be considered a vertical wall. It is the departure from this idealization that allows interaction between the shelf and oceanic flow.

1.2. Outline

In section 2 we discuss in detail the particular situation on the WFS and the motivation for the mathematical model presented in section 4 through two numerical experiments. In section 3, observations are shown to be consistent with the numerical model results presented in section 2. Section 4 contains an analytic solution for the evolving pressure at the shelf break, which is the juncture of two simple flow models: a geostrophic model for the deep ocean and a barotropic model with linear bottom friction on the shelf (termed the arrested topographic wave (ATW) by *Csanady* [1978]). To address concerns raised in section 4, a slightly more complicated set of equations is solved numerically in section 5 to assess the role of advection of momentum. Concluding remarks are offered in section 6.

2. Numerical Model Results

2.1. Reduced Gravity Model Results

A recent study by *Pichevin and Nof* [1997] demonstrates, with the use of an integrated momentum constraint, that a current configured like the Gulf of Mexico Loop Current cannot be maintained in steady state and must shed eddies. For mathematical simplification this study ignores the presence of the WFS. To examine the effects of a landmass in the place of the WFS, a reduced gravity numerical model identical to the one used by *Pichevin and Nof* [1997] is run with the addition of two vertical walls placed to represent the WFS. A snapshot of the calculated depth field after a steady state is achieved is shown in Figure 1. At this point the model has been integrated 2000 days without any eddy shedding; the model appears to be in a steady state. The difference between this result and the *Pichevin and Nof* [1997] study lies in the presence now of a northward flowing jet along the WFS. The leakage of mass to the north halts eddy shedding if the northward jet carries a sufficient amount of mass (momentum) away from the impinging Loop Current.

The presence of the northward wall jet has indeed been

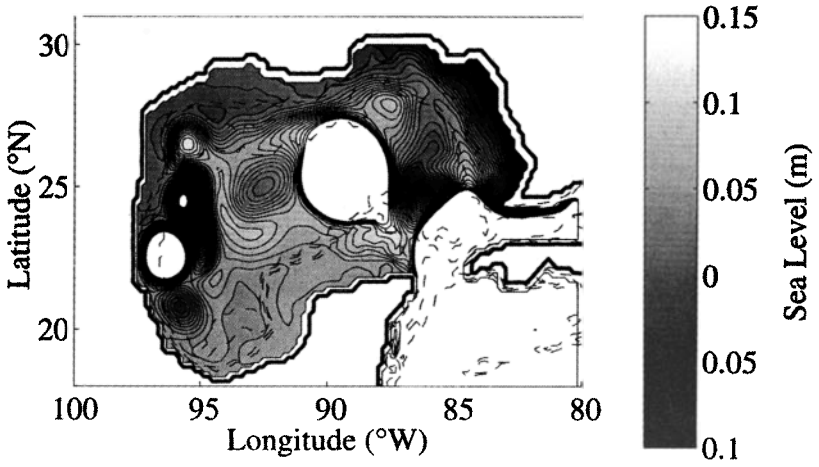

Figure 2. Contours of (approximate) sea level height. Results are from a numerical model of the Gulf of Mexico. The contour interval is 0.01 m. Contours of high sea surface height in the Loop Current eddy and within the Loop Current are not included in order to highlight the sea level variations over the shelf and slope.

explained by considering an integrated momentum balance [*Whitehead*, 1985]. The portion of the Loop Current that impacts the wall does so at an angle. If the entire flow along the wall were directed to the south, there would have been an imbalance in meridional momentum, since the incoming flow would have less southward momentum than the outgoing flow along the wall and a steady state would have been impossible. For a steady state balance to be possible the meridional momentum of the incoming flow must be equal to the sum of that of both the northward and southward flowing wall jets. Thus there is the need for the northward flowing wall jet along the WFS.

It should be noted that if the wall representing the WFS is moved eastward, that is, if the longitudinal spacing between the source and wall is increased, eddy shedding is modified but not halted. Moving the wall eastward influences the angle at which the northern limb of the Loop Current impacts the WFS: the greater the distance between the inflow port and the WFS, the smaller the angle between the northern Loop Current limb and the wall and the weaker the northward flowing jet. Apparently, there is a critical value of the northward transport along the wall for which greater transport shuts down the eddy shedding process. One theory for explaining the initiation of eddy shedding is that as the thermocline in the center of the loop deepens, the westward drift due to the β effect increases and forces the loop to break away and to form an eddy. If the northward transport along the WFS wall is enough to prevent the thermocline in the center of the loop from deepening, no eddy will be formed. Thus both the presence and the magnitude of this northward jet in the reduced gravity model seem to fundamentally alter the dynamics and behavior of the modeled Loop Current, although it is not clear exactly how.

2.2. Three-Dimensional Model Results

The effect of a sloping continental shelf instead of a vertical wall is examined with the aid of a fully three-dimensional (3-D) numerical model of the Gulf of Mexico based on the Geophysical Fluid Dynamics Laboratory (GFDL) model (also used by Hsueh and Golubov, submitted manuscript, 2001). The model is driven only with inflow and outflow conditions (30 Sv into the Gulf through the Yucatan Strait and out through the Straits of Florida) and surface relaxation of temperature and salinity to climatological values; no wind stress is applied. The simulated Loop Current sheds eddies regularly, with a period of ~9 months. Results show that when the Loop Current has not penetrated far into the Gulf of Mexico, a couple of months after a previous eddy has been shed, there is a tongue of high-pressure anomaly along the western edge of the WFS, with pressure decreasing to the north (see Figure 2). The pressure anomaly along the 300-m isobath is plotted in Figure 3 so that the decay of the tongue may be seen in more detail.

In Figure 4, cross sections of meridional velocity and temperature show the vertical structure of the tongue. The meridional currents appear to be in the geostrophic balance anticipated from the temperature cross section; the boundary between the northward and southward flow at the shelf break occurs at the trough in temperature just seaward of the shelf break (coincident with the dynamic pressure high in Figure 2).

Clearly, the presence of a shelf instead of a wall fundamentally changes the dynamics of the northward flowing jet arising from contact of the Loop Current with the WFS. In the reduced gravity case with a vertical wall the structure of the jet remains unchanged as it flows north. In the case with realistic topography with a sloping shelf the jet stays seaward of the shelf break and decays as it flows northward, eventually disappearing altogether, and the along-shelf extent of the high-pressure tongue associated with the jet is finite. The southward flowing jet on the shelf, ostensibly caused by Loop Current-imposed pressure at the edge of the WFS [*Hetland et al.*, 1999], appears to be fed by the northward flowing jet seaward of the shelf break.

3. Observational Evidence

3.1. Hydrography

Observational evidence also supports the idea of a local high in pressure along the shelf break when the Loop Current is young (with small northward penetrations). A hydrographic survey on the WFS at 26°N (Figure 5) shows that temperature and density (σ_t) both have depressions at roughly the 200-m isobath, corresponding to a high in dynamic topography. Comparisons with Figure 4 show that the overall structure is reproduced in the GFDL numerical model calculations.

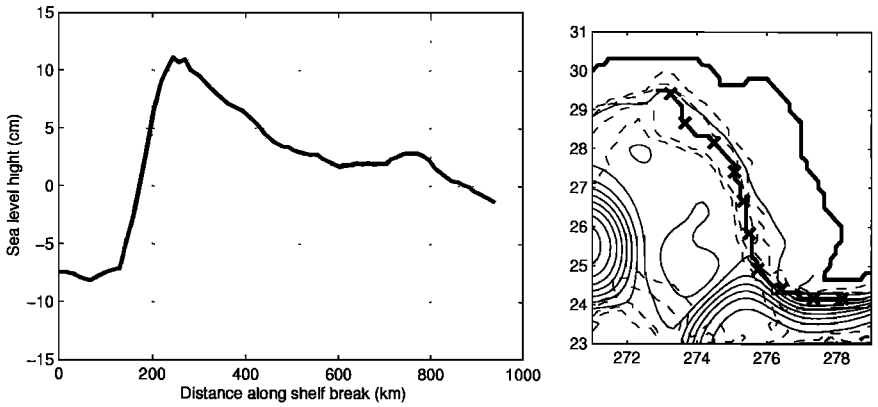

Figure 3. (left) Pressure plotted against distance along the 300-m isobath. (right) Path of the 300-m isobath, beginning in the southeast corner and continuing to the northwest. Crosses are plotted every 100 km along the path for comparison to the abscissa. Dashed lines denote isobaths at 100, 200, 1000, and 2000 m. Contours of sea surface height (thin, solid lines with a contour interval of 10 cm) are given so that the point where the Loop Current impacts the WFS may be inferred.

There is a middepth maximum of salinity on the shelf, which must have origins in the Loop Current. A high-salinity pool on the shelf is also noticed by *Niiler* [1976], who attributes its presence to intrusions from the Loop Current. A Loop Current eddy was shed 3 months prior to *Price and Mooers'* [1975] survey [*Vukovich*, 1988], so that the Loop Current has not had sufficient time to develop and is thus in a young stage. This suggests that the high-salinity pool is not due to intrusions of Loop Current filaments [*Paluszkiewicz et al.*, 1983] but is due to advection of Loop Current water from the south. The high-salinity pool is thicker where the inferred geostrophic flow is northward and thinner where the inferred geostrophic flow is southward, placing the source in the northward flowing jet. The implication is that the southward flow on the shelf is fed, in part, by the northward flow farther offshore, causing the northward flow to decay.

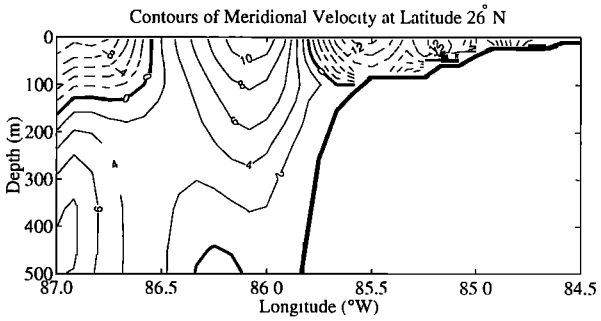

(a) Velocity.

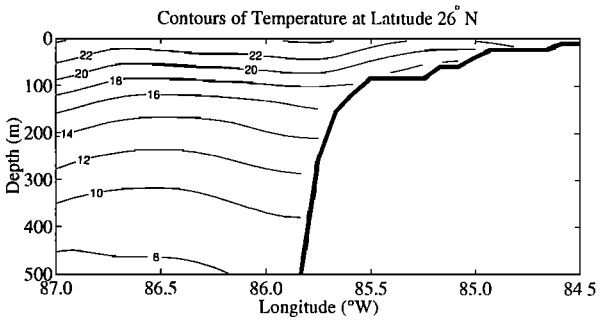

(b) Temperature.

Figure 4. Cross section of the tongue shown in Figure 2 at 26°N. Isotherms are depressed along the edge of the shelf, corresponding to the jet flowing north along the shelf. The eastern edge of a Loop Current eddy is seen on the far left.

3.2. Advanced Very High Resolution Radiometry Imagery

Satellite data confirm the presence of a northward flowing jet arising from the bifurcation of the Loop Current. Figure 6 shows two advanced very high-resolution radiometry (AVHRR) images taken February 1 and 3, 1997. Darker shades represent warmer water. In both images a filament of warm water can be seen to extend north from the Loop Current (the large pool of warm water in the south), along the shelf edge. Although it is difficult to ascertain flow directions from AVHRR images, it seems plausible that the filament must have originated from the Loop Current and extended to the north, since only the Loop Current water has such a high temperature. Thus the inferred flow direction of the warm water filament is to the north. Since warm water is typically associated with high dynamic pressure, the warm filament is also most likely associated with a high-pressure tongue (similar to that in Figure 2 from the GFDL model).

4. Analytical Model

4.1. Equations

The influence of a sloping shelf instead of a vertical wall on the shoreward side of a baroclinic jet can be illustrated by joining together two simple models. In the deep ocean a flat bottom, geostrophic flow model is the simplest representation of the dynamics. On the shelf a barotropic model is used, with linear bottom friction added, since bottom friction is found to be important to the shelf circulation over the timescales of interest [*Hetland*, 1999; *Hetland et al.*, 1999]. Although the deep ocean solution is degenerate, friction on the shelf breaks

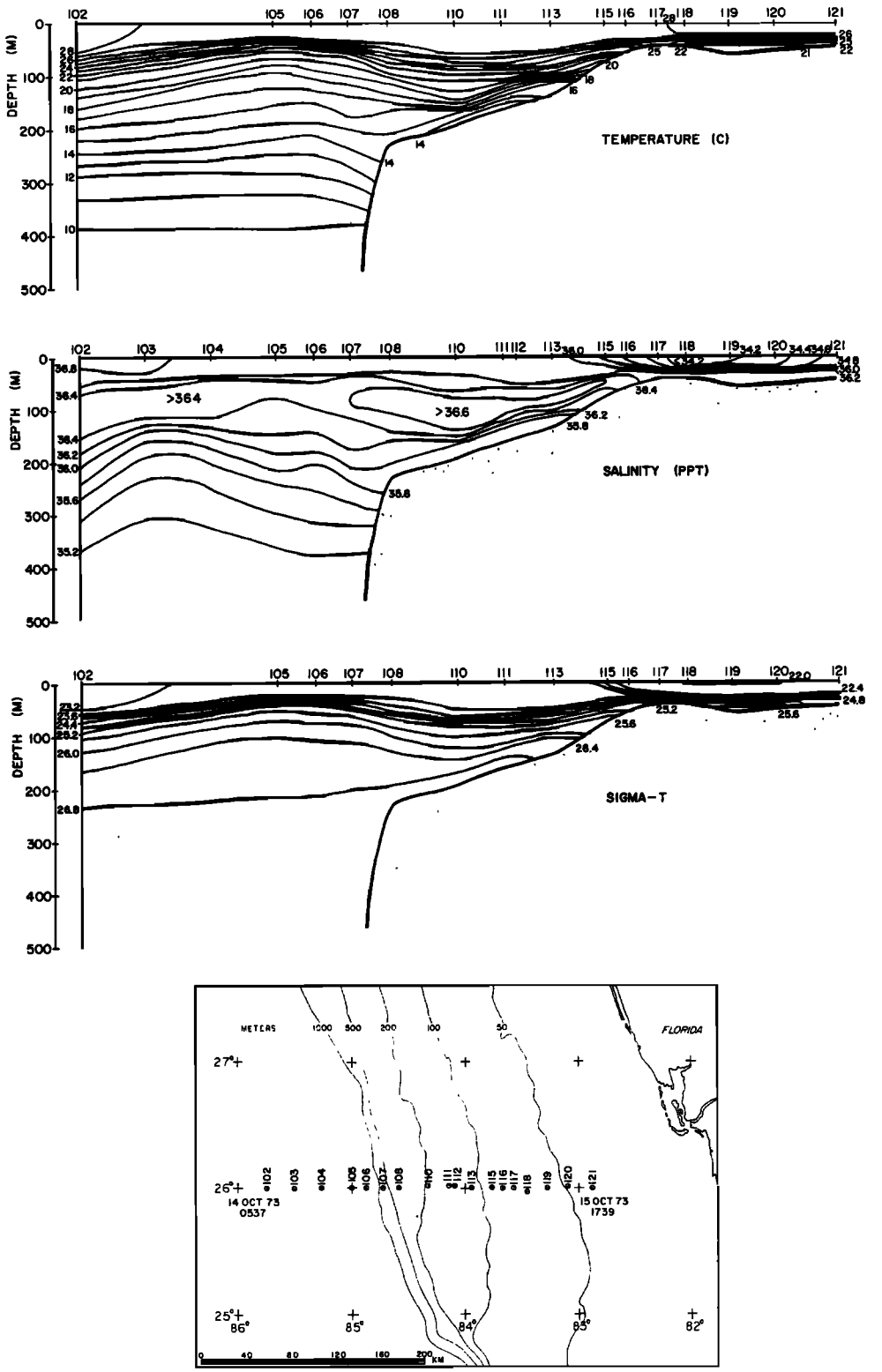

Figure 5. Hydrographic profiles of temperature, salinity, and σ_t cross section at 26°N on the WFS, taken October 14–15, 1973 [from *Price and Mooers*, 1975]. Profiles clearly show a depression in all fields at approximately the 200-m isobaths.

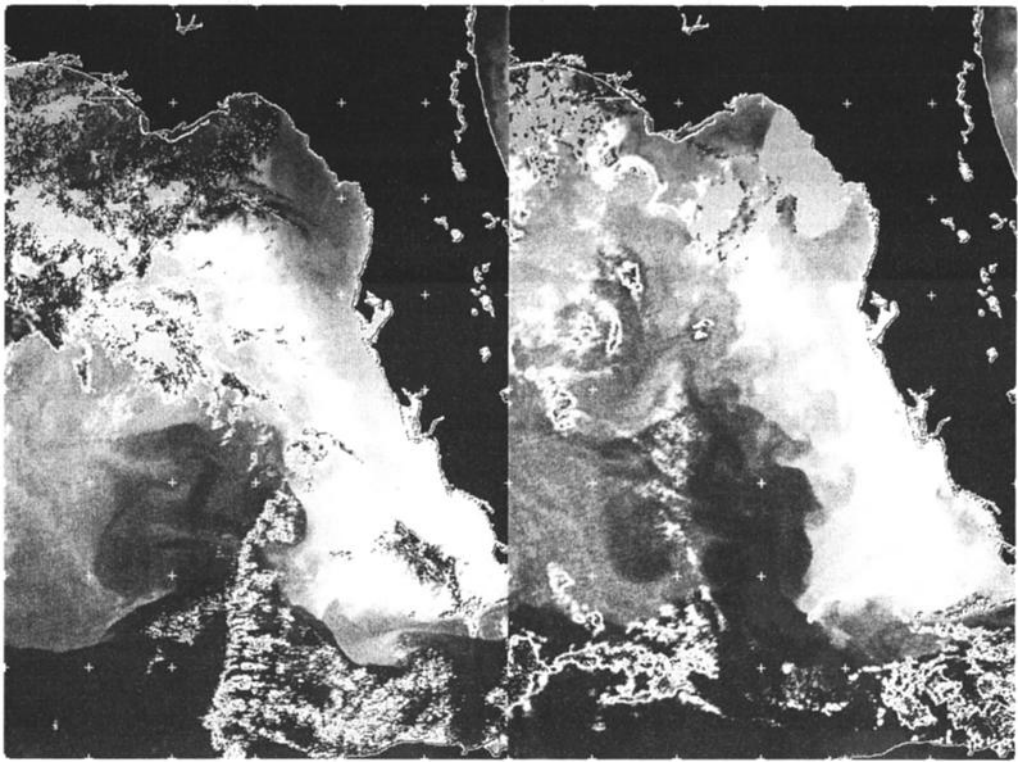

Figure 6. Advanced very high resolution radiometry (AVHRR) images from (left) February 1, 1997. (right) February 3, 1997.

the geostrophic degeneracy, and the circulation everywhere on the shelf can be calculated unambiguously.

In deep water (to the left of the shelf in Figure 7) a linear, constant depth, geostrophic model is used, so that the equations of motion are

$$-fv_1 = -g\zeta_{1x} \tag{1}$$

$$fu_1 = -g\zeta_{1y} \tag{2}$$

$$u_{1x} + v_{1y} = 0, \tag{3}$$

where f is the coriolis parameter and g is the gravitational standard. Notice that (1)–(3) are identical to those for a reduced gravity model in which the thermocline displacements are considered small compared with the mean thermocline depth H_0 of the deep ocean. The anomalous deep ocean sea level displacement about the mean sea level is represented by ζ_1 (positive upward), and the along- and cross-shelf velocities are represented by v_1 and u_1, respectively. On the shelf (to the right of the step in Figure 7) a barotropic flow model is used:

$$-fv_2 = -g\zeta_{2x} \tag{4}$$

$$fu_2 = -g\zeta_{2y} - \frac{rv_2}{h} \tag{5}$$

$$(u_2h)_x + hv_{2y} = 0, \tag{6}$$

where $h(x)$ is the cross-shelf depth field. Here, u_2 and v_2 are the like velocities on the shelf, ζ_2 is the sea level height anomaly on the shelf, and r is a constant bottom friction coefficient.

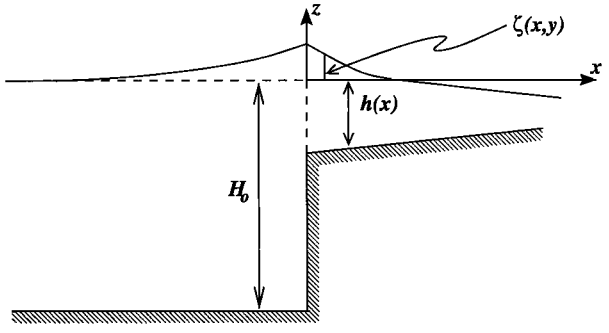

Figure 7. An idealized configuration of a baroclinic jet flowing along the edge of a continental shelf. The mean position of the thermocline in the deep ocean is H_0 below the surface, and thermocline displacements (positive downward) are represented by $\eta(x, y)$. Sea level height anomalies on the shelf are represented by $\zeta(x, y)$. The along-shelf coordinate, y, is positive into the paper.

4.2. Applications

4.2.1. Deep ocean. In the deep ocean, only a particular solution may be found because of geostrophic degeneracy. It is important to note that because of geostrophic degeneracy, pressure at the edge of the shelf will only matter to the particular solution. The particular solution in the deep ocean may be approximated by assuming that cross-shore scales are much smaller than along-shore scales. In this case, sea level decays exponentially away from the shelf break, or

$$\zeta_1 = \zeta_1(0, y)e^{x/R}, \tag{7}$$

where R is the baroclinic radius of deformation. For the Gulf of Mexico, $R \sim 50$ km. As it turns out, the details of the deep ocean solution do not affect the shelf solution, and the value of

R will only be important when appending an oceanic solution to the shelf.

4.2.2. Arrested topographic wave (shelf). A general equation for ζ_2 on the shelf may be found by substituting (4) and (5) into (6) results in the following equation referred to as the "arrested topographic wave" [see *Csanady*, 1978]:

$$\zeta_{2y} + \frac{r}{fh_x}\zeta_{2x} = 0, \tag{8}$$

where to keep the problem manageable, h_x will be taken to be a (negative) constant. It has been shown [*Hetland*, 1999; *Hetland et al.*, 1999] that (8) is a reasonable approximation of the dynamics of the WFS under the long timescales presently considered. Equation (8) has the form of the diffusion equation, with the timelike variable being positive y and a "diffusivity constant"

$$\kappa \equiv -\frac{r}{fh_x}. \tag{9}$$

4.2.3. Boundary condition at the shelf break. At the shelf break ($x = 0$) the two models are joined by the following boundary conditions. Continuity requires that the cross-shelf transports are equal, so

$$u_1(0, y)H_0 = u_2(0, y)h_0, \tag{10}$$

where $h_0 \equiv h(0)$. Also, the pressure must be continuous at $x = 0$:

$$\zeta_1(0, y) = \zeta_2(0, y). \tag{11}$$

Equations (2), (5), and (10) can be used to find the relation

$$\zeta_{2y}(0, y) = \kappa\alpha\zeta_{2x}(0, y), \tag{12}$$

where $\alpha \equiv -h_x/(H_0 - h_0)$. The remainder of the solution deals only with ζ on the shelf, so the subscript 2 will subsequently be dropped.

4.2.4. Initial conditions at $y = 0$. Values of ζ at $y = 0$ are required to find a solution. For simplicity, let

$$\zeta(x, 0) = \begin{cases} Z_0 & x = 0, \\ Z_1 & x > 0. \end{cases} \tag{13}$$

Constant values are chosen for simplicity.

For the WFS case, $Z_1 \sim -Z_0$ is a good approximation (see Figure 3). The low pressure on the shelf (i.e., negative Z_1) is consistent with the Loop Current riding up onto the shelf south of the "stagnation point," the point at which the Loop Current impacts the shelf. According to the Bernoulli principle the stagnation point, where there is no velocity, corresponds to a high dynamic pressure (see Figure 3). In the analytic model the stagnation point occurs at $y = 0$. The increased current speed along the shelf south of the stagnation point, caused by a constriction of the Loop Current as it approaches the Straits of Florida, creates a low dynamic pressure, again, according to the Bernoulli principle (see Figures 2 and 3). This phenomenon is discussed in more detail by *Hetland* [1999].

4.2.5. Solution. Equation (8), with boundary conditions (12) and (13) in addition to finite sea level height conditions at the coast, may be solved using the Laplace transform method. Equation (8) is transformed in y, as is the boundary condition at the shelf break (equation (12)). After inversion [see *Erdélyi*, 1954, equation (5.6.16)] the following solution is found:

$$\zeta(x, y) = (Z_0 - Z_1)\exp(\kappa\alpha^2 y + \alpha x) \cdot \operatorname{erfc}\left(\frac{x}{\sqrt{4\kappa y}} + \alpha\sqrt{\kappa y}\right) + Z_1. \tag{14}$$

A solution is plotted in Figure 8, with parameters typical for the WFS and adjacent waters. Qualitatively, the solution compares favorably with the numerical model results shown in Figure 2.

At the shelf break the solution reduces to

$$\zeta(0, y) = (Z_0 - Z_1)\exp\left[\frac{\kappa h_x^2 y}{(H_0 - h_0)^2}\right]\operatorname{erfc}\left[-\frac{h_x\sqrt{\kappa y}}{(H_0 - h_0)}\right] + Z_1. \tag{15}$$

The same solution shown in Figure 8 is shown at the shelf break ($x = 0$) in Figure 12. Again, the structure of the solution compares favorably with numerical calculations (see Figure 3).

Insight into the qualities of the solution may be gained by following the heat/conduction analogy. Equation (8) with boundary condition (12) represents a finite, homogeneous reservoir of heat attached to the end of a semi-infinite rod. The size of the reservoir is inversely proportional to α. Thus, for an infinite reservoir ($\alpha = 0$) the temperature of the reservoir never changes, and there is simply a fixed temperature at the end of the rod. It can be seen that (14) and (15) reduce to the appropriate form in this limit. If the reservoir is finite, as heat leaks into or out of the neighboring rod, the reservoir temperature changes accordingly.

4.2.6. Critique. An unsatisfying feature of solution (14) is the appearance in Figure 8 of broken contours at the shelf break. The cross-shelf derivative of pressure is not continuous; that is, there is a discontinuity in along-shore velocity across the topographic step. While the broken contour seems local and benign, it points to a fundamental deficiency of the linear model in that there must be a region that bridges the two simple flow models across the topographic step in which the change in water column height is allowed. The dynamics in such an intervening region may be highly nonlinear and quite intractable, although the along-shore velocity will be continuous across the step [*Spitz and Nof*, 1991]. Thus, strictly speaking, the shelf break condition (10) and subsequent results are valid only for a vanishingly small amount of flow across the shelf break.

5. Semigeostrophic Arrested Topographic Wave Numerical Model

To address the concerns brought up in the critique of the analytical model, a numerical model is used to solve an equation set, with nonlinear (and time-dependent) terms included in the along-shore equation. In this case, it is possible to resolve the slope region dynamics and to remove the discontinuity at the shelf break. The results can then be compared to evaluate the assumptions made in the analytical model.

The extended equation set used is

$$-fv = -g\eta_x, \tag{16}$$

$$v_t + uv_x + vv_y + fu = -g\eta_y - rv/h, \tag{17}$$

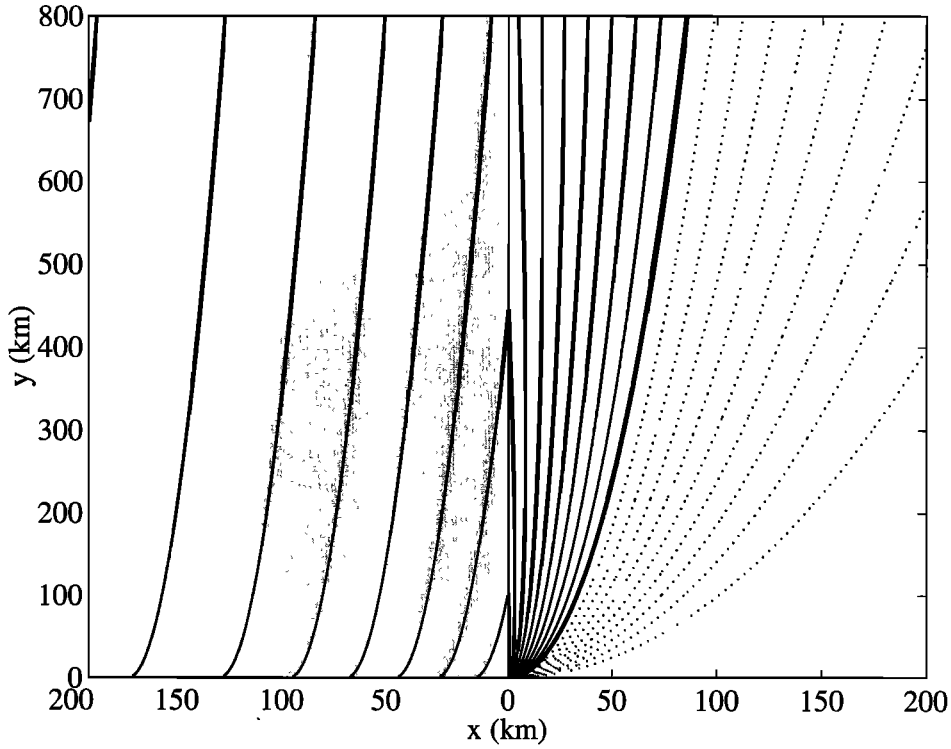

Figure 8. The analytical solution for $\zeta(x, y)$ contoured with constants representative of the WFS region: $r = 2 \times 10^{-4}$ m s^{-1}, $h_x = -2.5 \times 10^{-4}$, $H_0 = 350$ m, $h_0 = 150$ m, and $f = 6 \times 10^{-5}$ s^{-1}. The sea level in the deep ocean (shaded) is approximated by exponential decay away from the shelf break, with a decay scale of 50 km. Nondimensional sea level height ranges from $Z_0 = 1$ to $Z_1 = -1$. The thick solid line is the zero contour, thin solid lines are positive contours, and dotted lines are negative contours. The contour interval is 0.1.

$$(uh)_x + v_y h = 0. \tag{18}$$

To distinguish it from the other numerical models, the steady state solution of (16)–(18) will be referred to as the semigeostrophic arrested topographic wave (SGATW). In this case, the notation is identical to that used in section 4, except that here, $r = r(x)$.

Equations (16)–(18) can be combined to form a vorticity equation:

$$q_t = -(uq_x + vq_y) + [q + f]\frac{uh_x}{h} - \left[\frac{rv}{h}\right]_x, \tag{19}$$

where

$$u = -\frac{\Psi_y}{h}, \tag{20}$$

$$v = \frac{\Psi_x}{h}, \tag{21}$$

$$q = v_x = \left[\frac{\Psi_x}{h}\right]_x. \tag{22}$$

The approximation of relative vorticity, q, as the cross-shelf shear in along-shelf velocity is typical in coastal settings where the geometry determines that along-shelf flow is much stronger than cross-shelf flow. Notice that (19) can be rewritten in a more traditional form as

$$\frac{D}{Dt}\left[\frac{q+f}{h}\right] = -\frac{1}{h}\left[\frac{rv}{h}\right]_x, \tag{23}$$

(where D/Dt is the total derivative) which states that potential vorticity is modified along a streamline only by friction.

Equation (19) is solved numerically in ψ, with the other variables calculated diagnostically from the solution. The domain for (19) is a channel, shown in Figure 9, with $\psi(x, 0)$

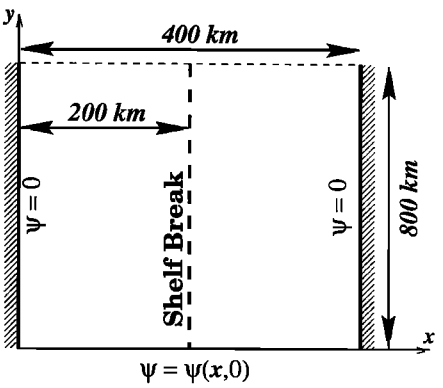

Figure 9. The domain used in the semigeostrophic arrested topographic wave (SGATW) numerical model calculation is a channel, open to the north, with ψ specified at the southern boundary.

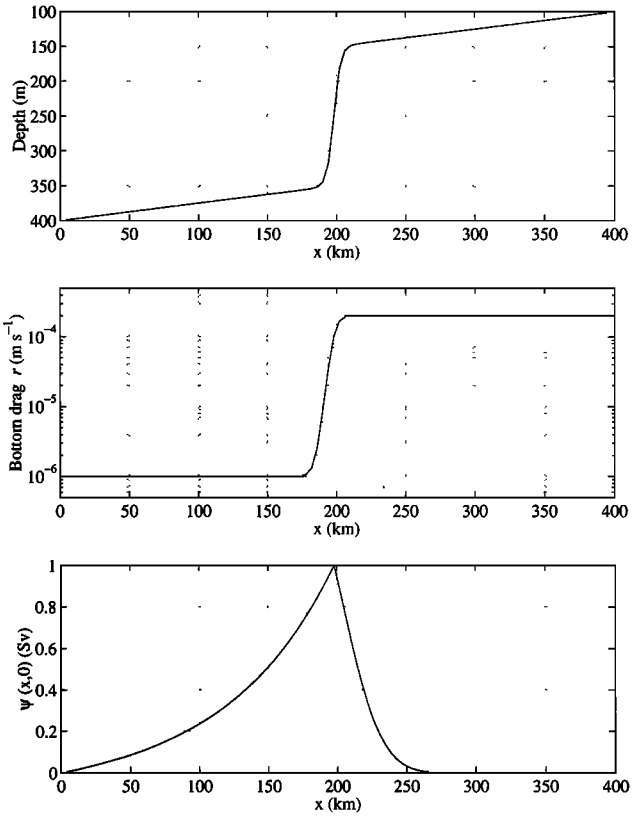

Figure 10. Various, specified cross-shore functions used in the SGATW numerical calculation.

specified on the southern boundary, with $\psi(0, y) = \psi(L, y) = 0$ (L is the channel width shown in Figure 9) at the eastern and western boundaries, and with an open northern boundary. The particular form of $\psi(x, 0)$ was chosen so the numerical solution might be compared to the analytical solution derived in section 4.2.5. Over the shelf the southern boundary condition, $\psi(x, 0)$, was chosen to match the form of the analytical solution 20 km from the initial step (i.e., $\zeta(x, 20\text{ km})$) to avoid a discontinuity. In the deep ocean, ψ decays exponentially, with a decay radius of 75 km from its value over the slope. The stream function boundary condition was normalized so that there is 1 Sv of transport in both the northward and southward jets at the southern boundary. The depth h, the friction coefficient r, and the stream function specified along the southern boundary are shown in Figure 10. Again, these values are chosen to facilitate comparison with the analytical model. The topographic gradients and bottom friction on the slope are identical. In the deep ocean, bottom friction is decreased 2 orders of magnitude, so that friction is negligible in this region.

A snapshot of sea surface elevation, well after the model has reached a steady state after 300 days of integration, is shown in Figure 11. A tongue of high sea level can clearly be seen along the shelf break at $x = 200$ km. Qualitatively, this compares favorably to the surface elevation field (shown in Figure 8). The major differences in the two solutions are caused by (1) the presence of a continental slope region in the numerical model, causing the sea level values to merge smoothly between the shelf and the deep ocean, and (2) southward advection of vorticity in the numerical model, causing the stream function contours on the shelf to be gathered southward near the southern end of the shelf.

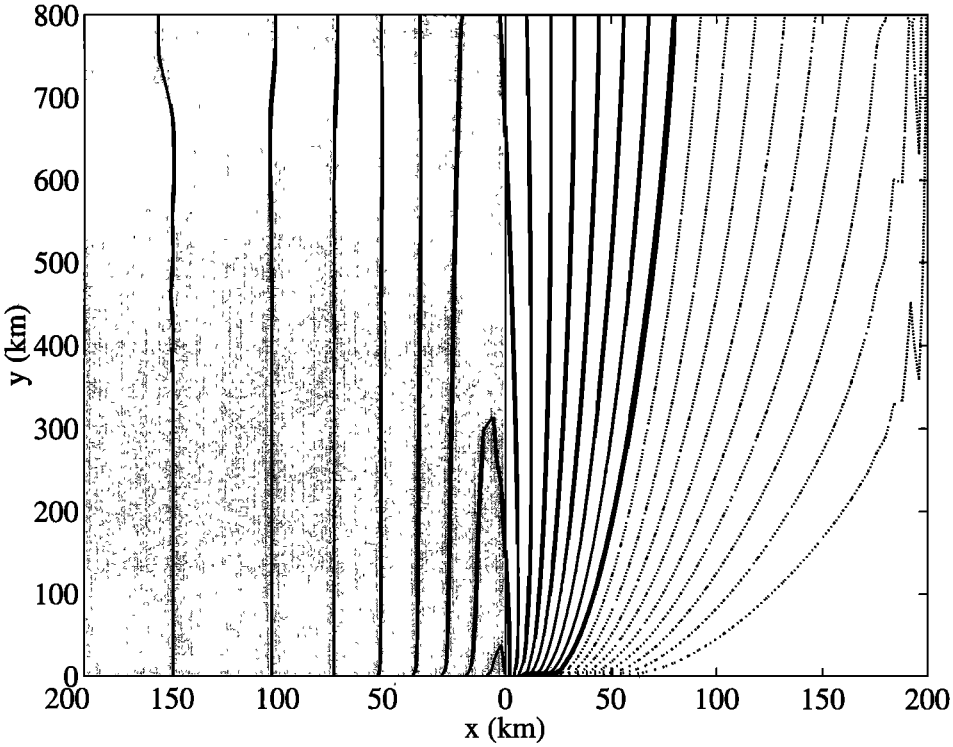

Figure 11. Numerical solution of the sea surface height field over the entire domain after the model has reached a steady state (300 days of integration). Actual values range from −0.02 to 0.02 m, with a contour interval of 0.002 m. Negative contours are dotted lines and the zero contour is a solid bold line, allowing for direct comparison to Figure 8.

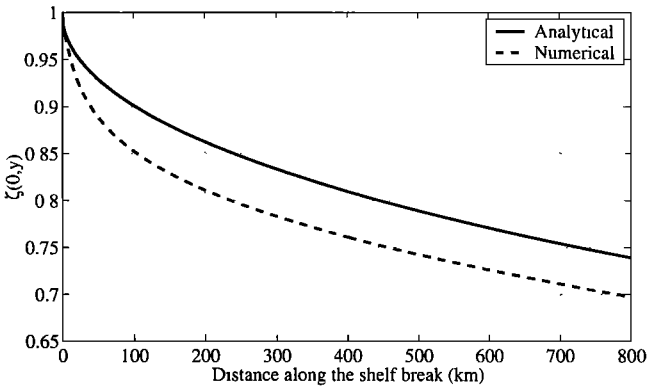

Figure 12. Comparison of the analytical and numerical (SGATW) sea surface height values at the shelf break (see Figures 8 and 11).

The cross-shelf flow associated with the strong gradients in along-shelf sea surface height violate the original assumption that the relative vorticity may be approximated by v_x. This is caused by a discrepancy between the imposed stream function structure along the southern boundary and what the interior stream function would set there if the boundary was allowed to adjust. However, in this model it is assumed that the Loop Current is setting the southern pressure field, so the stream function along the southern boundary is considered immutable. Thus the numerical solution is only valid outside the narrow region where the interior solution adjusts to the imposed southern boundary condition. The excellent agreement with the analytical model in the valid region indicates that while advection may be important mathematically in the matching boundary conditions between the deep ocean and the shelf, it does not fundamentally alter the structure of the solution.

Sea surface elevations at the shelf break, as calculated by the analytical and SGATW numerical models, are compared in Figure 12. There is very good agreement between the analytical and numerical results away from the southern boundary; the sea level gradients are nearly identical. Again, near the southern boundary, there are differences due to the southward advection of vorticity on the shelf in the region where the reliability of the SGATW model is questionable.

A plot of the term balance for the SGATW numerical model (Figure 13) shows that the result is dynamically similar to that found with linear ATW theory. Over the continental slope, there is strong horizontal shear in the along-shore currents, causing a large negative relative vorticity in this region, which is balanced by bottom friction. This balance is identical to linear ATW theory. The large negative relative vorticity is associated with a weak onshore flow (see Figure 13) over the slope, while weak positive relative vorticity over the shelf is associated with offshore flow.

As the width of the slope approaches zero, which is the idealization of the analytical model, the relative vorticity will become infinite. This will allow onshore flow over the slope despite very large topographic gradients. In the limit of zero width, there is a discontinuity in the along-shore velocities, and a nonzero cross-shelf velocity at the shelf break. Thus the problem of discontinuous along-shore velocity in the analytical model is a natural limit of the more complicated problem in which a slope is included.

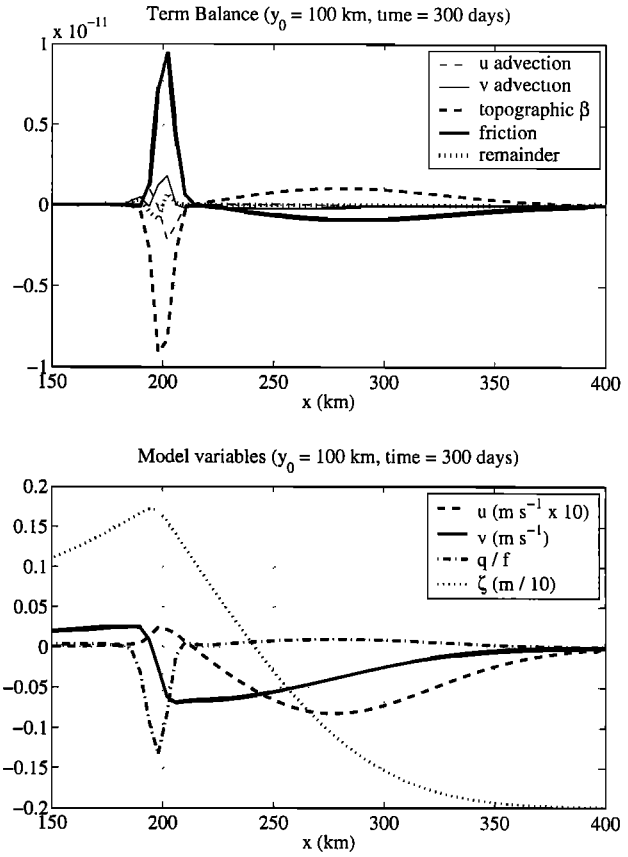

Figure 13. (top) Term balance for the SGATW numerical model. The dominant balance is between the "topographic β" term $[(q + f)uh_x/h)]$ and the "friction" term $[(rv/h)_x]$. (bottom) Various diagnosed model variables, calculated from the stream function field. Notice that the range of x has been reduced to focus on the shelf/slope region.

6. Conclusion

A comparison of a 3-D (GFDL) model and a reduced gravity numerical model of the Loop Current suggests that interaction between the Loop Current and the West Florida Shelf (WFS) is fundamentally altered if the WFS is represented by a wall instead of by realistic topography. In both cases the Loop Current bifurcates, and a northward flowing jet is formed along the seaward edge of the shelf. In the case in which the WFS is represented by a wall this northward flowing jet removes mass from the growing Loop Current, and eddy shedding is apparently halted. In the case in which realistic topography is used to represent the WFS the jet leaks mass onto the shelf, which joins a southward shelf flow formed in response to the deep ocean jet.

It is hard to gauge the exact influence of realistic topography on eddy shedding dynamics. However, on the basis of a comparison between the GFDL and reduced gravity models, there is good reason to believe that the inclusion of some form of shelf topography fundamentally changes the nature of eddy shedding in the Gulf of Mexico. The return flow on the shelf may restore enough mass to the growing loop so that the Loop Current penetration is never halted. In this manner, the shelf may play an unanticipated role in the eddy shedding process. The transport onto the shelf from the deep ocean (the "leakage" of the deep ocean jet), which is estimated to be ~1 Sv

integrated along the length of the shelf break, may also play a significant role in the salt, heat, and nutrient budgets on the shelf.

Although this paper is concerned with a very particular case in a local region, the theory developed is sufficiently general that it could be applied to any region in which strong oceanic currents interact with a continental slope. Warm-core rings hitting the Mid-Atlantic Bight shelf and the Kuroshio intrusion into Luzon Strait are examples in which the timescales are long enough and the deep oceanic flow is energetic enough to create significant cross-slope exchange due to frictional processes on the shelf.

Acknowledgments. The authors would like to thank Bill Dewar and Doron Nof for helpful comments and encouragement. This manuscript represents part of Robert Hetland's dissertation work at Florida State University, which was supported by the Minerals Management Service Cooperative Agreement 14-35-0001-30804.

References

Chapman, D. C., A simple model of the formation and maintenance of the shelf/slope front in the Middle Atlantic Bight, *J. Phys. Oceanogr.*, *16*, 1273–1279, 1986.

Chapman, D. C., and K. H. Brink, Shelf and slope circulation induced by fluctuating offshore forcing, *J. Geophys. Res.*, *92*(C11), 11,741–11,759, 1987.

Csanady, G. T., The arrested topographic wave, *J. Phys. Oceanogr.*, *8*, 47–62, 1978.

Csanady, G. T., and P. T. Shaw, The "insulating" effect of a steep continental slope, *J. Geophys. Res.*, *88*(C12), 7519–7524, 1983.

Erdélyi, A., *Tables of Integral Transforms*, vol. I, McGraw-Hill, New York, 1954.

Hetland, R. D., The dynamics of a Loop Current forced shelf break jet on the West Florida Shelf, Ph.D. thesis, Fl., State Univ., Tallahassee, 1999.

Hetland, R. D., Y. Hsueh, R. R. Leben, and P. P. Niiler, A Loop Current-induced jet along the edge of the West Florida Shelf, *Geophys. Res. Lett.*, *26*, 2239–2242, 1999.

Li, Z., and R. H. Weisberg, West Florida Shelf response to upwelling favorable wind forcing: Kinematics, *J. Geophys. Res.*, *104*(C6), 13,507–13,527, 1999.

Middleton, J. H., Steady coastal circulation due to oceanic alongshore pressure gradients, *J. Phys. Oceanogr.*, *17*, 604–612, 1987.

Niiler, P. P., Observations of low-frequency currents on the West Florida Continental Shelf, *Mém. Soc. R. Sci. Liège*, *X*, 331–358, 1976.

Paluszkiewicz, T., L. P. Atkinson, E. S. Posmentier, and C. R. McClain, Observations of Loop Current frontal eddy intrusion onto the West Florida Shelf, *J. Geophys. Res.*, *88*(C14), 9639–9651, 1983.

Pichevin, T., and D. Nof, The momentum imbalance paradox, *Tellus Ser. A*, *49*, 298–319, 1997.

Price, J. F., and C. N. K. Mooers, Shelf dynamics fall experiment October–December '73 hydrographic data, technical report, Rosenstiel Sch. of Mar. and Atmos. Sci., Univ. of Miami, Miami, Fla., 1975.

Shaw, P.-T., and C.-Y. Peng, A numerical study of the propagation of topographic Rossby waves, *J. Phys. Oceanogr.*, *17*, 358–366, 1987.

Spitz, Y. H., and D. Nof, Separation of boundary currents due to bottom topography, *Deep Sea Res., Part A*, *38*(1), 1–20, 1991.

Sturges, W., The spectrum of Loop Current variability from gappy data, *J. Phys. Oceanogr.*, *22*, 1245–1256, 1992.

Sturges, W., The frequency of ring separations from the Loop Current, *J. Phys. Oceanogr.*, *24*, 1647–1651, 1994.

Vukovich, F. M., Loop Current boundary variations, *J. Geophys. Res.*, *93*(C12), 15,585–15,591, 1988.

Welsh, S. E., The response of a steep shelf to deep-ocean forcing, Master's thesis, Fl., State Univ., Tallahassee, 1986.

Whitehead, J. A., The deflection of a baroclinic jet by a wall in a rotating fluid, *J. Fluid Mech.*, *157*, 79–93, 1985.

R. Hetland, Department of Oceanography, Texas A&M University, College Station, TX 77845-3146. (rhetland@tamu.edu)

Y. Hsueh, Department of Oceanography, Florida State University, Tallahassee, FL 32306. (hsueh@re.ocean.fsu.edu)

D. Yuan, SSAI, Inc., 5900 Princess Garden Parkway, Suite 300, Lanham, MD 20708. (dyuan@janus.gsfc.nasa.gov)

(Received January 13, 2000; revised September 29, 2000; accepted December 15, 2000.)